Nuclear Instruments and Methods in Physics Research B 119 (1996) 445–451

ELSEVIER

NIM B
Beam Interactions with Materials & Atoms

Stopping powers of 200–3000 keV ^{4}He and 550–1750 keV ^{1}H ions in Vyns

F. Munnik, A.J.M. Plompen, J. Räisänen [1], U. Wätjen *

Institute for Reference Materials and Measurements (IRMM), CEC-JRC, Retieseweg, B-2440 Geel, Belgium

Received 2 July 1996

Abstract

Stopping powers for Vyns (vinylchloride-vinylacetate copolymer) were measured both for ^{4}He ions in the range 200–3000 keV and for ^{1}H ions in the range 550–1750 keV using the transmission technique. A detector model is used for the energy calibration to improve the accuracy of the stopping power curve for ^{4}He ions in the low energy region. The estimated uncertainty in the stopping power values is ~1.5% for ^{4}He ions and ~2% for ^{1}H ions. A comparison is made between a parametrization of the present data and several parametrizations of the stopping power found in the literature. The stopping power values closest to the present experimental data for ^{4}He ions are obtained by adding elemental stopping powers using Bragg's rule. For this the experimental values for the Cl stopping power reported earlier should be used. The charge state scaling, sometimes used to take account for phase-state effects, is not appropriate for Vyns. For ^{1}H ions, the parametrization closest to our data is that of Janni from 1982.

Keywords: Stopping power; Helium; Hydrogen; Polymers; Vyns

1. Introduction

The stopping power of light ions in polymers is of considerable interest due to their use in various ion beam applications, e.g. as absorber, exit foil, backing material and detector window. Another important interest in the stopping power of these materials originates in radiation safety and radiology from their similarity to human tissue. Stopping power data for a sufficient set of these materials also give information about stopping power additivity rules which are needed for the accurate extrapolation of stopping powers to new composite materials and tissue. In the present work the body of stopping power data for polymers is extended with a Cl containing compound.

The objective of the present study is to determine the stopping powers for ^{1}H and ^{4}He ions in Vyns (vinylchloride-vinylacetate copolymer) in an energy range interesting for ion beam applications, including the stopping power maximum for ^{4}He ions. The method chosen for this work is the transmission technique [1–3]. Since the foils used in these experiments are rather small, the mass is small and it is difficult to obtain accurate areal densities. Therefore, we have normalized our data to a reference stopping power value for ^{4}He ions obtained previously by using a ^{148}Gd source on a set of larger foils with accurate areal densities. A detailed discussion is given of the analysis procedure including the use of a model for the detector response in order to reduce the influence of day-to-day fluctuations in the energy calibration on the stopping-power curve, especially at and below the stopping-power maximum. To our knowledge, there are no other experimental data for ^{1}H and ^{4}He ions on Vyns available. A comparison to various widely used parametrizations and models for the stopping power [4–8] is presented. This work is part of a systematic study of stopping powers in (co)polymers [3].

2. Experimental procedure

Thin Vyns foils are prepared at our institute by dissolution of pellets of 90% vinylchloride – 10% vinylacetate random copolymer (Union Carbide) in cyclohexanon and subsequent centrifugation on glass plates [9]. The foils are then transferred onto Al rings with 5 mm inner diameter. The nominal areal density of the foils is 45 μg/cm^2, additional values of 90 and 135 μg/cm^2 are obtained by double and triple stacking these foils. Henceforth the areal density is also called thickness t since for stopping power measurements the areal density is the most useful quantity to describe the

* Corresponding author. Tel. +32 14 571211, fax +32 14 584273, e-mail watjen@pixe.irmm.jrc.be.

[1] Permanent address: Accelerator Laboratory, Department of Physics, P.O. Box 43, FIN-00014 University of Helsinki, Finland.

PII S0168-583X(96)00468-5

"thickness" of a sample. The stoichiometry $(H_{33}C_{22}O_2Cl_9)_n$ for Vyns is found by adding the stoichiometry of vinylacetate to nine times the stoichiometry of vinylchloride which is a valid method for random copolymers.

The experimental arrangements for the energy loss determination are described briefly below and are given in detail in Ref. [3]. The $^1H^+$ and $^4He^+$ beams for the energy loss measurements were produced by the 3.7 MV Van de Graaff accelerator of the IRMM. The beam energy is determined with a 90° analyzing magnet and a calibrated nuclear magnetic resonance (NMR) probe (see Ref. [3]). The accuracy of the NMR probe calibration is ~1 keV. The day-to-day reproducibility of the analyzing magnet is 2–3 keV. The beam is collimated to 0.5 mm diameter and scattered at an angle of 165° from a scatterer. The spread in the detected energy due to variations in scattering angle is limited to ~0.5 keV by beam collimation. The scatterers are polished disks of vitreous-C, Al, Ni or Au. The scattered particles are registered by a 50 mm^2 passivated implanted planar silicon (PIPS) detector collimated by a 6 mm Ta diaphragm. Just in front of the detector and 75 mm from the scatter target there is a collimator wheel holding the foil stacks and a spare empty Al ring, used for the blank measurements. The spectra are collected in 8k channels with a count rate not exceeding ~4.5 kcps to prevent shifts in the edges due to pile-up. For the proton measurements the single foil has not been used because the energy loss is very small resulting in large uncertainties. This effect also limits the upper energy of the proton beams for the other foil stacks to about 1.8 MeV.

A reference stopping power was obtained earlier by using a ^{148}Gd source emitting α-particles of 3183 keV. The foils were about 5 cm in diameter and were prepared as described above. The areal density was determined by microbalance weighing and area determination. The energy loss of the α-particles was subsequently measured at five positions using the method described in Refs. [10]. The average results of these measurements for each foil are presented in Table 1 since they were not published previously. The uncertainty in the energy loss in the foil E_{loss} is the standard deviation of the five measurements. The uncertainty of 20 keV in the average energy $\overline{E} = (E_{bl} + E_{fl})/2$, with E_{bl} and E_{fl} the energies of the blank and foil edges respectively, is caused by the energy loss in the source and in the detector window. These energy losses do not contribute to the uncertainty in E_{loss} of the foils since they are identical for the blank and foil measurements. Only the asymmetrical part of the energy straggling in the foil can lead to a shift in the energy distribution after passing the foil. This contributes to the error in E_{loss} but since the straggling in the foils is small and much less than the detector resolution this effect can be neglected [3,11]. The values for $\overline{E}$ and the stopping power S are calculated using Eqs. (5) which are valid for these foil thicknesses and energy. Calculating the weighted average of these results yields a reference stopping power S_{ref} = 0.996 (10) MeV cm^2/mg at E_{ref} = 3141 (20) keV.

Table 1
Measurements with a ^{148}Gd alpha-source used for the determination of a reference stopping power. The thickness t is determined by weighing and area determination. The uncertainty in t is 1 $\mu g/cm^2$. The energy loss in the foil, E_{loss}, is the average of five measurements with the standard deviation as uncertainty. The third and fourth column are determined using Eqs. (5)

t [$\mu g/cm^2$]	E_{loss} [keV]	$\overline{E}$ [keV]	S [MeV cm^2/mg]
45	42.4 (5)	3161.8	0.942 (23)
83	83.9 (9)	3141.1	1.010 (16)
138	138.5 (16)	3113.7	1.004 (13)

3. Analysis

The first step in the analysis is the fitting of the spectra to obtain the position of the edges. A detailed discussion of this procedure is given in Ref. [3]. The uncertainty in the edge position is ~1–2 channels for ^{4}He and ~0.4–1.2 channels for ^{1}H.

The next step is the energy calibration. The blank measurements (no foil) have been used for the energy calibration of the detector. For protons a linear fit is sufficient to describe the detector response. An energy calibration is made for each measuring day separately, with at least three beam energies per day. The uncertainty in the fit parameters for the conversion from channels to energy is about 0.3%. For ^{4}He ions the energy calibration is complicated by the non-linear detector response below ~2 MeV. Simply using a higher order polynomial is not necessarily sufficient to describe this non-linearity and, in particular, it does not eliminate day-to-day variations of the stopping power curve below the maximum. As the energy calibration turned out to be very critical for the stopping power curve at and below the maximum, a different approach is used to take the detector response into account.

When the response of the detection electronics is sufficiently linear to use a linear relation between the detected energy E_{det} and the channel number c in the spectrum, the energy calibration is described by Eq. (1), where E_P is the true energy of the detected particle, a_0 and a_1 are the parameters of the linear fit, and E_{PHD} is the term describing the non-linear detector response given by Eq. (2).

$$E_P = a_0 + a_1 c + E_{PHD}(E_P), \tag{1}$$

$$E_{PHD}(E_P) = \Delta E_{win}(E_P)\left(1 + \frac{k}{\varepsilon_0} S(E_P)\right) + \Delta E_n(E_P)\left(1 + \frac{k}{\varepsilon_0} S(E_P)\right) - \frac{k}{\varepsilon_0}\int_0^{E_P} S(E)\,dE. \tag{2}$$

Here, ΔE_{win} is the energy loss in the detector dead layer and window, ΔE_n is the energy defect caused by non-ionizing

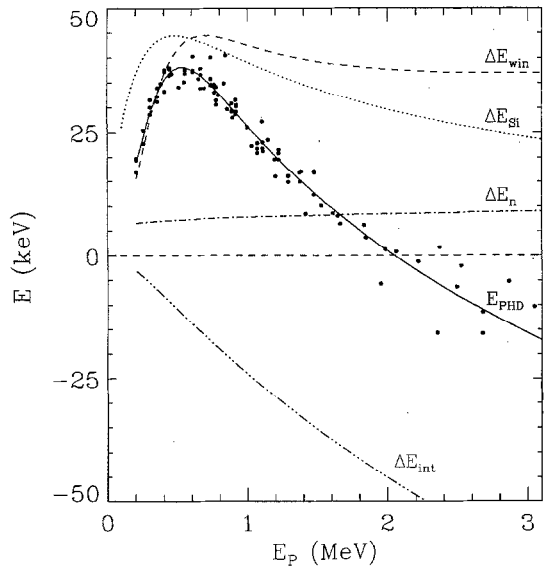

Fig. 1. The total pulse height defect E_{PHD} and its constituents as a function of energy. The dots are E_{PHD} calculated by using Eq. (1). The solid line is E_{PHD} calculated by using Eq. (2). The dashed line is a fit of energy loss in the window ΔE_{win}. The dashed-dotted line (ΔE_n) is the energy defect caused by non-ionizing processes. The dashed-triple dotted line (ΔE_{int}) represents the dependence of the electron–hole pair creation energy on the ionization density (the last term with the integral in Eq. (2)). The dotted line (ΔE_{Si}) is the stopping power curve for Si from Ref. [6] normalized to the height of ΔE_{win}.

processes, i.e. by nuclear collisions, ε_0 is the electron–hole pair creation energy (3.67 eV as measured for X-rays), k a constant (see below), and $S(E)$ the stopping power in Si. With this calibration function day to day variations in the electronics result in different values for a_0 and a_1 for each day. However, the term $E_{PHD}(E_P)$ is determined solely by the detector characteristics and is therefore common to all measuring days. Note that E_{PHD} also depends on the bias voltage since a partially depleted detector was used [12] but the bias voltage was always kept identical.

Eq. (2) is derived from a function introduced by Lennard et al. [13] (Eq. (3)), for which support is found in a growing number of publications [14,15,12,16].

$$E_{det} = \varepsilon_0 \int_0^{E_P - \Delta E_{win} - \Delta E_n} \frac{dE}{\varepsilon_0 - kS(E)}. \tag{3}$$

The term $kS(E)$ makes ε a function of the ionization density in the detector. This is needed to explain the dependence of E_{det} on the Z of the detected particle [13]. The factor k is determined by Bauer and Bortels to be $2.8(3)10^{-4}$ nm/electron–hole pair [15]. Since $kS(E)/\varepsilon_0 \sim 10^{-2}$ and ΔE_{win} and ΔE_n are small compared to E_P, Eq. (3) can be simplified. Using the linear relation between E_{det} and c Eqs. (1) and (2) are derived.

The term ΔE_n is calculated using the simulation program TRIM92 [6] for selected energies and a fourth order polynomial is used for interpolation. The integration term in Eq. (2) is evaluated numerically using the k of Bauer and Bortels [15] and the stopping power for Si from Ref. [6]. The term ΔE_{win} should be proportional to the stopping power of Si and some effective dead-layer thickness. However, if we try to determine the dead-layer thickness with the Si stopping power, the value for the thickness becomes unphysically large. This is caused by the fact that the shape of the experimental ΔE_{win} does not resemble the Si stopping power curve very well. Therefore, we have tried to extract a ΔE_{win} curve from our calibration data as described below. It should be remembered that the only aim of this exercise is to obtain a reliable and reproducible energy calibration of our detector. The values for ΔE_{win} can be extracted from the calibration data and then fitted using a function describing the stopping power curve. For this, an iterative procedure is needed since the amplifier gain was maximized for each measuring day. This procedure consists of several steps. In the first step E_{PHD} is calculated; for the first iteration ΔE_{win} is taken zero. Next the linear calibration (Eq. (1)) is performed for each measuring day separately. Using the fit parameters, an experimental energy loss for the window can be calculated. In the last step, all ΔE_{win}^{exp} are combined and fitted with the function described below by Eq. (6). These steps are repeated until the change in ΔE_{win} is negligible. This final result gives a good description of the energy calibration data of all measuring days. The values for E_{PHD} and its components are shown in Fig. 1. The uncertainty s_{a_1} in the fit parameter a_1 of Eq. (1) is ~0.16%.

It should be noted that ΔE_{win} in Fig. 1 does not resemble the stopping power curve of Si derived from Ref. [6] or the other parametrizations used in this work very well. This could be explained by the fact that the detector surface is contaminated, e.g. by C–H compounds commonly present in vacuum systems, or it may reflect a non-uniform Si dead-layer. Furthermore, it should be remembered that the term ΔE_{win} calculated in this way may also contain effects not taken into account by the model of Lennard et al. [13].

Once the correct energy calibration is obtained, the energies of the edges are determined. The energy loss is then the subtraction of the energies of the blank and foil edges ($E_{bl} - E_{fl}$). For the ^{1}H measurements, this can be simplified to: $E_{loss} = a_1(c_{bl} - c_{fl})$ with c_{bl} the edge position of the blank measurement and c_{fl} the edge position of the measurement with foil. The uncertainty $s_{E_{loss}}$ in E_{loss} is now also straightforward:

$$s_{E_{loss}} = \left(E_{loss}^2 \left(\frac{s_{a_1}}{a_1} \right)^2 + 2a_1^2 s_c^2 \right)^{1/2}, \tag{4}$$

with s_{a_1} the uncertainty in a_1 and s_c the uncertainty in both c_{bl} and c_{fl}. For the ^{1}H measurements, this leads to an uncertainty of 0.5–2.2% depending on the energy loss. The calculation of E_{loss} for ^{4}He is more complicated but Eq. (4) is still a good approximation, leading to an uncertainty of 0.2–1.4% depending on the energy loss. The relative uncer-

tainty for ^{4}He is smaller than for ^{1}H because the energy loss is much larger.

In the final step of the analysis, the stopping power and the average energy can be calculated according to

$$S(\overline{E}) \approx E_{\mathrm{loss}}/t. \tag{5}$$

$$\overline{E} = \frac{E_{\mathrm{bl}} + E_{\mathrm{ft}}}{2}.$$

The square of the relative uncertainty in S is the sum of the squares of the relative uncertainties in E_{loss} and t. This formula is only valid for small energy losses. For each thickness, the average energy is calculated at which the stopping power calculated according to Eq. (5) differs more than 1% from the stopping power at this average energy. The Ziegler–TRIM stopping powers [6] are used for this calculation. The energies thus found are 69 keV for the single foil, 255 and 462 keV for stacks of two and three foils respectively. Measurements with $\overline{E}$ below these values are excluded. Measurements with an average energy below the lowest calibration point are also excluded. This procedure is only necessary for ^{4}He ions since the energy loss for ^{1}H ions in the used energy range is sufficiently small to guarantee the validity of Eqs. (5).

Instead of using an independently determined thickness, the reference stopping power $S_{\mathrm{ref}}(E_{\mathrm{ref}})$ given in Section 2 is used to determine the thickness. In our case, this is more accurate than weighing and area determination because the masses and areas of the present foils are very small. To obtain precise values for the thickness from the reference stopping power, first the E_{loss} curves are fitted using the following equation (see Ref. [3]):

$$E_{\mathrm{loss},i}(E) = b_i E^{a_1} \frac{1 + a_2 E + a_3 E^2}{1 + a_4 E^2 + a_5 E^3}. \tag{6}$$

The parameters $a_1 \ldots a_5$ are obtained by a fit of the E_{loss} curves of all three foil stacks simultaneously which are normalized using the nominal thicknesses of the foil stacks. The denominator does not contain a term proportional to E to reduce the number of free parameters. The one parameter less does not result in any loss of accuracy of the fit. The parameters b_i are then obtained by fitting each E_{loss} curve individually and keeping $a_1 \ldots a_5$ fixed. Only the high energy part (>1.75 MeV) of the curves is used for the fit because in this way the fit is more stable at the energy (3.141 MeV) for which the reference stopping power is determined. The thicknesses for each foil stack are $t_i = E_{\mathrm{loss},i}(E_{\mathrm{ref}})/S_{\mathrm{ref}}(E_{\mathrm{ref}})$ with $E_{\mathrm{loss},i}(E_{\mathrm{ref}})$ calculated using Eq. (6). The thicknesses thus obtained are 45.4 (5), 91.5 (10), and 136.0 (15) μg/cm^2 for the one, two, and three foil stacks respectively. Iterating this procedure with these thicknesses as starting values does not change the results significantly. The thicknesses are also used for the ^{1}H ion measurements.

4. Results and discussion

The stopping power results for ^{4}He and ^{1}H ions are displayed in Figs. 2 and 3 respectively. The total uncertainty in the stopping power is in the range of 1.1–1.8% for ^{4}He and 1.2–2.5% for ^{1}H. The curve in Fig. 2 is a fit to the data using Eq. (6). The average deviation of the data for ^{4}He ions from the parametrization is 0.8%. This value, being a measure for the statistical uncertainty in the measurements, is in

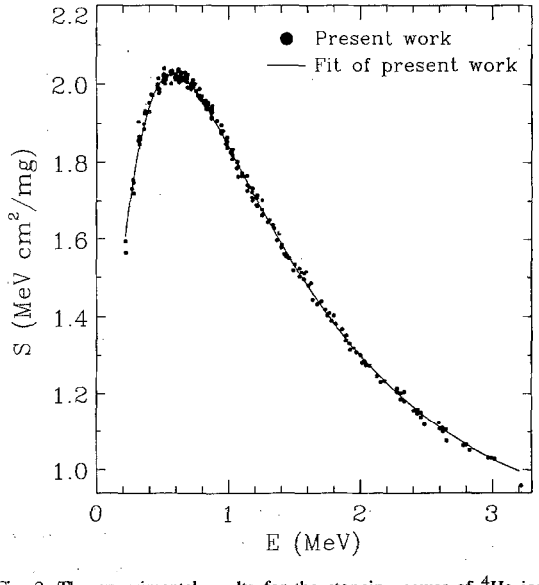

Fig. 2. The experimental results for the stopping power of ^{4}He ions in Vyns. The full curve is a fit to Eq. (6). The parameters are $a_0 = 2.548$, $a_1 = 0.3737$, $a_2 = 0.9990$, $a_3 = -0.2403$, $a_4 = 1.826$ and $a_5 = -0.3920$ with E in MeV and S in MeV cm^2/mg.

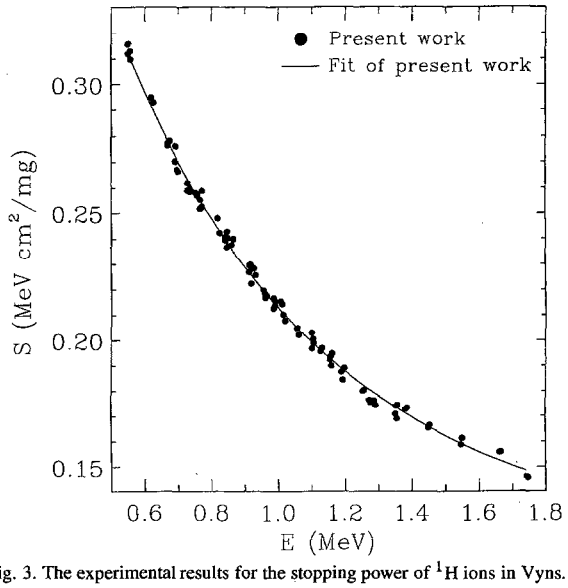

Fig. 3. The experimental results for the stopping power of ^{1}H ions in Vyns. The full curve is a fit to a fourth order polynomial with coefficients 0.5980, −0.7731, 0.5699, −0.2149 and 0.03297 with E in MeV and S in MeV cm^2/mg.

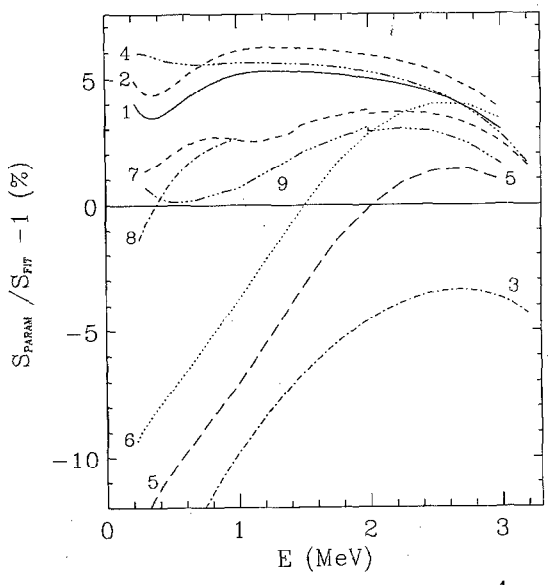

Fig. 4. The parametrization of Fig. 2 (S_{fit} in this figure) for ^{4}He ions compared to several parametrizations and models (S_{param}) given in the literature. The comparisons are: 1: TRIM code, parametrization using Bragg's rule [6]; 2: TRIM code, parametrization using the CAB model [6,7]; 3: Ziegler 77 scheme for solids [4]; 4: Ziegler 77 scheme for gases [4]; 5: ICRU report 49 for polyvinylchloride [8]; 6: ICRU report 49 using Bragg's rule [8]; 7: H, C and O from TRIM parametrization [6] and Cl from Powers et al. [17] below 2 MeV and Cl from Ref. [4] for gases above 2 MeV, added using Bragg's rule; 8: H, C and O from TRIM parametrization [6] and Cl from Baumgart et al. [18]; and 9: H, C and O from the ICRU report [8] and Cl as curve 7.

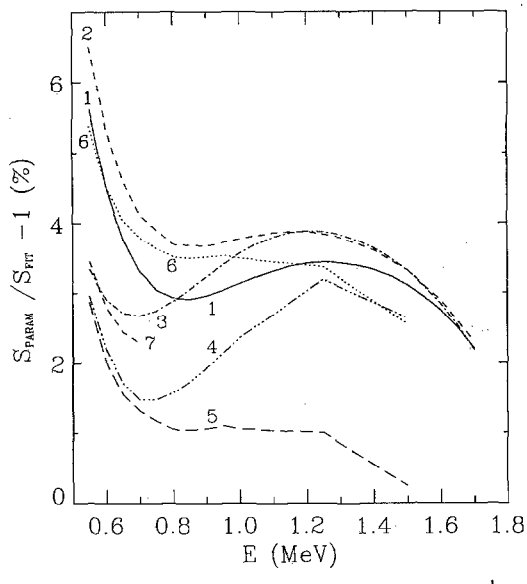

Fig. 5. The parametrization of Fig. 3 (S_{fit} in this figure) for ^{1}H ions compared to several parametrizations and models (S_{param}) given in the literature (cf. Fig. 4). Note that for protons Ref. [4] makes no distinction between gases and solids (curve 3). Curve 4 is the comparison with the stopping powers given by Janni [5]. Curve 7 is obtained in the same way as curve 8 in Fig. 4.

good agreement with the estimated uncertainty in E_{loss} (see section 3). The data for ^{1}H ions are fitted with a fourth order polynomial because the measurements do not include the stopping power maximum and therefore the parametrization of Eq. (6) is less suited. The average deviation of the data from the parametrization is 1.2%, again in good agreement with the estimated uncertainty in E_{loss}.

A comparison between the various parametrizations found in the literature and our results is given in Fig. 4 for ^{4}He ions and in Fig. 5 for ^{1}H ions. The literature schemes for ^{4}He ions are the Ziegler et al. parametrization as used in TRIM92 [6] both using Bragg's rule and the Cores and Bond model (CAB) [7] for summing individual contributions to the stopping power. The older Ziegler scheme [4] is included for both gases and solids. With the tabulated values for polyvinylchloride, H, amorphous C, and O from the ICRU report 49 [8], the stopping powers of Vyns are calculated according to Bragg's rule. The stopping powers for polyvinylchloride tabulated in that report were calculated using Bragg's rule, however the values for Cl used in that calculation are not tabulated. As can be seen from Fig. 4 none of the above parametrizations or models is in good agreement with the present data. Better agreement is obtained by adding experimentally obtained stopping values for Cl with the values of H, C, and O of the parametrizations according to Bragg's rule. The following combinations have been plotted: H, C, and O from Ref. [6] with Cl from Ref. [17] and with Cl from Ref. [18]; H, C, and O from Ref. [8] with Cl from Ref. [17].

For the TRIM code (curves 1 and 2 in Fig. 4), the values obtained with Bragg's rule are in better agreement with our data than the values obtained using the CAB model of that code, as was also found for polyimide [3]. The differences between the CAB model and Bragg's rule, however, are smaller than the difference between either and our data. A simulation calculation using TRIM92 (with Kinchin–Pease recoil/damage estimates) is also performed for both types of summation (not plotted in Fig. 4). The average deviations with our data are 5% for the simulation using Bragg's rule and 7.5% using the CAB model. There is no obvious reason why the difference between Bragg's rule and CAB model is much larger for the TRIM simulation than for the TRIM parametrization.

Vyns is a random copolymer of on average nine vinylchloride groups for each vinylacetate group. If this ratio is different by one vinylchloride group, the stopping power changes by less than 0.2% (using the TRIM stopping power [6] and Bragg's rule). This is not enough to explain the differences between the present data and the models and parametrizations in the literature. If the vinylacetate group is completely left out, polyvinylchloride is left over. The stopping power of this material according to Ref. [8] is about 3% lower than that of Vyns (compare curves 5 and 6 in Fig. 4). For $E > 1.5$ MeV, the polyvinylchloride stopping power is in good agreement with our data. However, such a large change

in composition can not be accounted for.

A possible explanation for the difference is that the stopping power values for Cl used in Refs. [4,6,8] are inaccurate. There is only one publication with experimental data for Cl containing compounds [17], all gases or vapors. The stopping power for Cl extracted from these data by Powers et al. [17] combined with the values for H, C, and O from Ref. [6] results in curve 7 in Fig. 4 for $E < 2$ MeV. Since these values are within 1% in agreement with the gas values from Ref. [4], the high energy part (>2 MeV) is obtained by using the gaseous Cl stopping powers from Ref. [4]. The difference between this scheme and our data is only 1–3%. The Cl stopping powers of Powers et al. and the gas values from Ref. [4] are also combined with the H, C, and O stopping powers of the ICRU report [8] (curve 9 in the figure) to give an even better agreement with the present data. There is also one publication from Baumgart et al. with experimental data for 100–1000 keV ^{4}He ions in gaseous Cl_2 [18]. Above 740 keV these data are in good agreement with Powers et al. [17] (less than 1%). Below this energy the difference increases to about 7% at 300 keV. The Cl stopping powers of Baumgart et al. are combined with the H, C, and O stopping powers from TRIM [6] to give curve 8 in Fig. 4. However, the chemical bonds of Cl in Vyns resemble the bonds of the molecules used by Powers et al. more closely than the bond in Cl_2, so the Powers et al. data are preferred.

The Cl stopping powers in TRIM [6] are obtained by interpolating from other elements. The values thus obtained are about 5% higher than the values from Powers et al. [17]. The TRIM stopping power of Cl would have to be decreased by about 12% to explain the whole difference between the TRIM stopping power using Bragg's rule [7] and the present data. The ICRU report [8] uses the Cl stopping powers for solids from Ref. [4] for energies below 1 MeV. Above 4 MeV it uses the Bethe theory. It interpolates in between these two energies. The gaseous stopping powers for Cl from Ref. [4] are based on the experimental values of Powers et al. [17] as can be concluded from the 1% agreement between the two. The solid stopping powers for Cl in Ref. [4] are based on the gaseous values and charge state scaling between gases and solids. In view of the large differences between our data and both the stopping powers for solids (curve 3 in Fig. 4) and the low energy part of the ICRU values (curve 6 in Fig. 4), it can be concluded that the charge state scaling as performed in Ref. [4] is inaccurate for Cl in Vyns and overestimates possible phase-state effects.

The difference between the best scheme in Fig. 4 (curve 9) and the present data, 0–3%, is within the stated uncertainties, which are 1.1–1.8% for the present work and 2.5–3.5% for the Cl stopping powers of Powers et al. [17], contributing about 1.3–1.8% to the stopping power of Vyns. This leaves little or no room for phase-state effects when uncertainties in H, C, and O are of the same order. This is consistent with the fact that for (co)polymers like Vyns, chemical effects on the additivity rule for stopping powers may be much larger than the phase-state effects since the polymer chains are only weakly bound.

The comparison for ^{1}H ions is made with the same parametrizations and models except that the Andersen and Ziegler scheme [4] makes no distinction between solids and gases and that the stopping powers of Janni [5] have been added. The ICRU values [8] are for our energy region completely based on the Bethe theory. In Fig. 5, the agreement between the present data and the literature is better than for ^{4}He ions, in the order of the combined stated uncertainties in the present work and in the literature. The stopping powers of Janni [5] have the smallest difference, ~1.5–3%, with stated uncertainties of 2–4%. In general, the remarks for ^{4}He ions also hold for ^{1}H. To explain the difference between the present data and the literature for ^{1}H ions, the Cl stopping power would have to be between 4 and 10% lower, depending on the literature scheme. The publication of Baumgart et al. [18] also contains data for 50–710 keV ^{1}H ions in Cl_2. Their values are about 1–4% lower than the stopping power values of Andersen et al. [4] between 100 and 700 keV. The Cl stopping power values of Baumgart et al. are combined with the H, C, and O values from TRIM [6] resulting in curve 7 in Fig. 5. The difference between our data and curve 7 is better than the TRIM parametrization (curve 1) but not as good as the Janni values (curve 4).

5. Conclusion

As a conclusion, it can be stated that the stopping powers of Vyns have been measured for ^{4}He ions in an energy range of 0.2–3 MeV and for ^{1}H ions in the range of 0.6–1.8 MeV with an accuracy of about 1.1–2.5%. To the knowledge of the authors no other experimental data exist for Vyns. The comparison of the experimental data with parametrizations and models in the literature showed differences of 3–8% for ^{4}He ions and 2–6% for ^{1}H. The smallest differences for ^{4}He ions, 0–3%, are obtained by adding the experimentally obtained stopping values for gaseous Cl [17] with the values of H, C, and O of Ref. [8] using Bragg's rule. The best scheme for ^{1}H ions is that of Janni [5], having differences with the present data of 1.5–3%. The differences with the literature can be largely explained by the use of inaccurate values for the Cl stopping powers. This is partly due to the limited knowledge of Cl stopping power values and partly due to the way in which the experimental values are included in the parametrizations. In view of the stated uncertainties, there is little room for phase-state effects when using ^{4}He ions, which is consistent with the weakly bound polymer chains. This may explain why the charge state scaling, used in Ref. [4] to account for phase-state effects, leads to large deviations with the present data.

The accuracy and reproducibility of the stopping power for ^{4}He at and below the stopping power maximum has been improved by using, in the energy calibration, the model for

the detector response described in Ref. [13]. This model is sufficient for a good energy calibration but it is no complete physical description of our detector. Possible improvements are better values for the Si stopping powers, a determination of the non-uniformity of the dead-layer and a better description of the integration term in Eq. (2) describing the dependence of the electron–hole pair creation energy on the ionization density.

Acknowledgements

We are grateful for the preparation of the Vyns foils by C. Ingelbrecht, R. Eykens and J. Van Gestel. In addition, we wish to thank M. Conti, A. Crametz, P. Falque, J. Leonard and W. Schubert for preparing the ion beams from the Van de Graaff Accelerator. J.R. is thankful for the financial support obtained as a visiting scientist under the CEC–JRC scheme. F.M. and A.P. each acknowledge a Human Capital and Mobility Grant issued by the European Commission.

References

[1] P. Mertens, Nucl. Instr. and Meth. B27 (1987) 315.
[2] J. Räisänen, U. Wätjen, A.J.M. Plompen and F. Munnik, Nucl. Instr. and Meth. B 118 (1996) 1.
[3] A.J.M. Plompen, F. Munnik, J. Räisänen and U. Wätjen, J. Appl. Phys. 80 (1996) 3147.
[4] H.H. Andersen and J.F. Ziegler, Hydrogen Stopping Powers and Ranges in All Elements;
J.F. Ziegler, Helium Stopping Powers and Ranges in All Elements;
Vols. 3 and 4 of: J.F. Ziegler (ed.), The Stopping Powers and Ranges of Ions in Matter (Pergamon, 1977).
[5] J.F. Janni, At. Data Nucl. Data Tables 27 (1982) 147.
[6] J.F. Ziegler, J.P. Biersack, U. Littmark, in: The Stopping and Range of Ions in Solids, ed. J.F. Ziegler (Pergamon, 1985);
J.F. Ziegler, TRIM92 computer code, private communication (1992)
[7] J.F. Ziegler and J.M. Manoyan, Nucl. Instr. and Meth. B 35 (1988) 215.
[8] ICRU report 49, Stopping powers and ranges for protons and alpha particles, International commission on radiation units and measurements (1993).
[9] J. Pauwels, J. Van Gestel, C. Vandecasteele and K. Strijckmans, Nucl. Instr. and Meth. A 236 (1985) 651.
[10] H.L. Eschbach, R. Werz, I.V. Mitchell and P. Rietveld, 8th Int. Vac. Congress, Cannes, 22–26 Sept. 1980;
H.L. Eschbach, R. Werz, I.V. Mitchell and P. Rietveld, Vakuum-Technik 30 (5) (1982) 142;
P. Rietveld, private communication.
[11] P. Sigmund and K.B. Winterbon, Nucl. Instr. and Meth. B 12 (1985) 1.
[12] W.N. Lennard and G.R. Massoumi, Nucl. Instr. and Meth. B 48 (1990) 47.
[13] W.N. Lennard, H. Geissel, K.B. Winterbon, D. Phillips, T.K. Alexander, and J.S. Forster, Nucl. Instr. and Meth. A 248 (1986) 454.
[14] W.N. Lennard and K.B. Winterbon, Nucl. Instr. and Meth. B 24/25 (1987) 1035.
[15] P. Bauer and G. Bortels, Nucl. Instr. and Meth. A 299 (1990) 205.
[16] W. Hösler and R. Darji, Nucl. Instr. and Meth. B 85 (1994) 602.
[17] D. Powers, W.K. Chu, R.J. Robinson and A.S. Lodhi, Phys. Rev. A 6 (1972) 1425.
[18] H. Baumgart, H. Berg, E. Huttel, E. Pfaff, G. Reiter and G. Clausnitzer, Nucl. Instr. and Meth. B 2 (1984) 145.